



Relationship between non-photochemical quenching efficiency and the energy transfer rate from phycobilisomes to photosystem II

Igor N. Stadnichuk¹ · Pavel M. Krasilnikov²

Received: 31 March 2023 / Accepted: 2 June 2023 / Published online: 16 June 2023
© The Author(s), under exclusive licence to Springer Nature B.V. 2023

Abstract

The chromophorylated PBLcm domain of the ApcE linker protein in the cyanobacterial phycobilisome (PBS) serves as a bottleneck for Förster resonance energy transfer (FRET) from the PBS to the antennal chlorophyll of photosystem II (PS II) and as a redirection point for energy distribution to the orange protein ketocarotenoid (OCP), which is excitonically coupled to the PBLcm chromophore in the process of non-photochemical quenching (NPQ) under high light conditions. The involvement of PBLcm in the quenching process was first directly demonstrated by measuring steady-state fluorescence spectra of cyanobacterial cells at different stages of NPQ development. The time required to transfer energy from the PBLcm to the OCP is several times shorter than the time it takes to transfer energy from the PBLcm to the PS II, ensuring quenching efficiency. The data obtained provide an explanation for the different rates of PBS quenching in vivo and in vitro according to the half ratio of OCP/PBS in the cyanobacterial cell, which is tens of times lower than that realized for an effective NPQ process in solution.

Keywords Chlorophyll · Energy transfer · Non-photochemical quenching · Orange carotenoid protein · Phycobilisome · Photosystem II

Abbreviations

APC	Allophycocyanin
FRP	Fluorescence recovery protein
FRET	Förster resonance energy transfer
hECN	3'-Hydroxyechinenone
NPQ	Non-photochemical quenching
OCP	Orange carotenoid protein
OCP ^O	Dark-stable orange form of OCP
OCP ^R	Photoactive red form of OCP
PBS(s)	Phycobilisome(s)
PE	C-phycoerythrin
PS II	Photosystem II
RCP	Red carotenoid protein

Introduction

Phycobilisomes (PBSs) are giant photosynthetic antenna complexes of phycobiliproteins consisting of disc-shaped ($\alpha\beta$)₃ polypeptide trimers and ($\alpha\beta$)₆ hexamers stacked into cylinders by a series of linker polypeptides and finally assembled into two structural domains: central core of allophycocyanin (APC) and the lateral rods of C-phycocyanin (PC) attached to the core and complemented by C-phycoerythrin (PE) or phycoerythrocyanin in some cyanobacterial species (Glazer 1994; Sidler 1994; Adir et al. 2019). The most studied hemidisoidal PBSs of the cyanobacterium *Synechocystis* sp. PCC 6803 (hereafter *Synechocystis*) have six PC peripheral rods and a triangular central core consisting of one upper and two parallel basal cylinders attached to the outer thylakoid surface of the photosystem II (PS II) dimers (Arteni et al. 2009; Bald et al. 1996; Chang et al. 2015; Dominquez-Martin et al., 2022; Kawakami et al. 2022; Xiao 2023). The direct or PS II mediated interaction of PBS with photosystem I remains controversial (Bald et al. 1996; Bryant and Canniffe 2018; Liu et al. 2013; Mullineaux 1994). The core contains two APC pigment groups, known as bulk APC trimers, which fluoresce at 660 nm, and trimers containing ApcE (Lcm), ApcD and ApcF polypeptides with

✉ Igor N. Stadnichuk
stadnichuk@mail.ru

¹ K.A. Timiryazev Institute of Plant Physiology, RAS,
Botanicheskaya 35, 127726 Moscow, Russia

² Biological Faculty of M.V., Lomonosov State University,
Lenin Hills 12, 119991 Moscow, Russia

red-shifted phycocyanobilin chromophores. Their fluorescence peaks, differ slightly, all around 680 nm (Capuano et al. 1991; Lundell and Glazer 1981; Gindt et al. 1994).

The excitation after light absorption is transferred in a cascade of energy transfer steps through multiple phycobilins from the lateral PC (or PE + PC) rods to the bulk APCs of the core, then to the long-wavelength phycobilins and finally to PS II with an efficiency of > 95% (Glazer 1994; Manodori et al. 1985). ApcE with its chromophorylated PBLcm domain fluorescing at 682 nm (at 77 K), plays the leading role in the long wavelength fluorescence emission of PBS and, as was first suggested in the study of the cyanobacterium *Nostoc* sp. MAC (Mimuro and Gantt 1986; Mimuro et al. 1986), provides the pathway for energy transfer to PS II. ApcF is located in the same APC trimer as the PBLcm domain and has auxiliary functions in relation to its chromophore at 682 nm. (Bald et al. 1996; Bryant and Canniffe 2018). APC trimers containing the ApcD polypeptide never show fluorescence longer than 679 nm in vitro, and it is most likely that ApcD is involved in energy delivery to PS I (Calzadilla et al. 2019; Dong et al. 2009; Liu et al. 2013; Mullineaux 1994).

The process of high-light adaptation in cyanobacteria, accompanied by a decrease in PBS fluorescence, is known as non-photochemical quenching (NPQ) (Rakhimberdieva et al. 2004; Wilson et al. 2006). This evolutionarily rather old (Bernát et al. 2012; Kerfeld et al. 2017; photoprotective phenomenon, induced by the orange carotenoid protein (OCP) (Wilson et al. 2006), reduces by quick thermal dissipation the amount of excess energy arriving from PBS at the antennal chlorophyll and then at the photosynthetic reaction centers (Rakhimberdieva et al. 2010). The 34–35 kDa OCP, with a single ketocarotenoid 3'-hydroxyechinenone (hECN) enclosed by N- and C-protein domains, exists in two distinct conformational states: an inactive, dark-stable orange form (OCP^O) and an active, metastable red form (OCP^R) generated by OCP absorption of intense blue-green light (Wilson et al. 2008). Most known cyanobacterial strains contain one OCP-encoding gene, while some, including *Nostoc punctiforme* (hereafter *Nostoc*), have two complete genes and several shorter paralogs (Boulay et al. 2008; Kerfeld et al. 2017).

PBS without bound OCP is not susceptible to NPQ; the estimated interaction of OCP^R with PBS in vitro (Gwizdala et al. 2011; Stadnichuk et al. 2011) had stimulated the search for a direct site of OCP binding to PBS in vivo. As *Synechocystis* mutants lacking lateral PBS cylinders showed similar amplitudes and rates of fluorescence quenching to wild-type cells (Scott et al. 2006; Stadnichuk et al. 2009; Wilson et al. 2008), the binding site was attributed to components of the PBS core. *Synechocystis* strains with deleted *apcD* and/or *apcF* genes retained the ability to induce the photoprotective mechanism (Jallet et al. 2012). Therefore, the search for the

quenching site focused on the remaining unexplored bulk APC and ApcE as part of the PBS core. In contrast to ApcD and ApcF, the role of the amorphous ~ 90 kDa ApcE protein in the cyanobacterial NPQ cannot be elucidated by whole gene knockout mutagenesis, as ApcE is essential for PBS assembly (Liu et al. 2005). The established in vitro interaction of OCP^R with purified ApcE and the apparent absence of OCP^R interaction with isolated bulk APC trimers strongly suggested that the ApcE must be the site of OCP^R action (Stadnichuk et al. 2012). The *Synechocystis* mutant lacking the PBLcm domain of ApcE loses its NPQ ability (Elanskaya et al. 2018). Another type of mutant with a deleted short loop inserted in PBLcm showed a twofold decrease in OCP-dependent PBS fluorescence quenching (Zlenko et al. 2019). Among the three identified cross-linked PBS-derived peptides closely involved in the OCP-PBS association, one contained a lysine belonging to ApcE (Zhang et al. 2014). These data provided the rationale for the subsequent modeling of the functional interaction between OCP and PBLcm. The spatial arrangements of the in silico models of OCP docking to the crystal bulk APC trimer(s) as well as to the APC trimer bearing the PBLcm domain were very similar, but in the case of PBLcm the model was more convincing due to fewer slits and steric clashes than the corresponding construction of OCP and bulk APC (Zlenko et al. 2016).

The non-covalent binding of OCP^R to PBS is reversible, making it difficult to maintain the in vivo attitude and to visualize possible microimages of the OCP-PBS super-complexes. Recently (Domiguez-Martin et al. 2021), the structure of the OCP-PBS complex was obtained in vitro with a resolution of 2.7 Å by cryo-electron microscopy. The images showed that the single PBS can interact with two OCP^R dimers at two different sites involving the bulk APC in the upper and lower cylinders of the PBS core. This appears to contradict the above evidence for PBLcm as site of OCP localization on the PBS surface in vivo. OCP-dependent NPQ in vivo and in vitro is achieved under very different conditions, forcing us to re-examine the in vivo and in silico NPQ data. Therefore, it has been controversial to date how PBS interacts with PS II and how OCP removes excess energy from PBS in high light. To this end, we have recorded fluorescence emission spectra during the entire process of NPQ formation in the pigment apparatus of the cyanobacterium *Nostoc* to obtain more evidence for the involvement of ApcE. This approach allowed us to detect the quenching of the 682 nm fluorescence band, indicating the direct involvement of ApcE in providing the NPQ effect in vivo.

The developed in (Krasilnikov et al. 2020) model of PBS docking to the PS II dimer on the surface of the thylakoid membrane was tested for the possibility of energy transfer via the PBLcm energy channel and for agreement between the calculated and experimental transfer times. The excitonic coupling model of the OCP and PBLcm interaction,

previously well established (Krasilnikov et al. 2020; Stadnichuk et al. 2015), was then revised in accordance with the course of energy transfer from PBLcm to PS II, as well as the PBS to OCP cell ratio. In this way, we show that, within the framework of the model constructed, the times of energy transfer from the PBLcm to the PS II and from the PBLcm to the OCP are closely correlated. We show that it is possible to reconcile the rates of energy transfer and the ratios of OCP, PBS and PS II present in cyanobacterial cells. This is based on the 682 nm fluorescence band, identified in our work, which is the first direct indication of the presence of PBLcm in the NPQ spectrum, and on corresponding calculations.

Methods

Strains and culture conditions

The PE-containing filamentous cyanobacterium *Nostoc punctiforme* ATCC 29133 (Hirose et al. 2010; Meeks et al. 2001) was grown for 5 days in BG-11 culture medium under constant white light of 35 $\mu\text{mol photons m}^{-2} \text{s}^{-1}$ and 30 °C with gentle stirring to partially break the filaments (Hirose et al. 2010). The unicellular cyanobacterium *Synechocystis* sp. PCC 6803 used to collect biomass for the isolation of OCP was grown in modified BG-11 medium containing double amount of sodium nitrate as described in (Elanskaya et al. 2018).

Fluorescence emission spectra

Fluorescence emission spectra of the *Nostoc* cell suspension were recorded at room temperature using a RF5301 PC spectrofluorimeter (Shimadzu, Japan) under excitation light at 520 nm, which is predominantly absorbed by PE. The optical density of the sample at the 678 nm red absorption maximum of chlorophyll was 0.1 in a 3 mm light path cuvette. The bandwidth of the excitation (photon flux density approximately 40 $\mu\text{mol photons m}^{-2} \text{s}^{-1}$) and measurement monochromators was 5 nm. The same 520 nm light, increased to 450 $\mu\text{mol photons m}^{-2} \text{s}^{-1}$, was used to induce NPQ by phototransformation of OCP^O to OCP^R with the slit of the excitation monochromator maximally open and a neutral filter removed from the light path. Specifically, it is an order of magnitude higher than light for the realization of State 1/ State 2 transitions (Calzadilla and Kirilovsky 2020). The total illumination time for the NPQ development was successively 0+30+30+60+60 s, with corresponding immediate spectral recordings lasting repeatedly 6 s. This time difference between the spectral recording and the NPQ development allowed us to use only one sample of the cell suspension in the fluorimeter holder in the continuity of the measurements and to record sequentially the intensity changes of all the revealed spectral

bands. Fluorescence spectrum of PBLcm with emission peak position at 682 nm was obtained by deconvolution of the PBS core fluorescence spectrum recorded and described previously (Stadnichuk et al. 2015).

OCP absorption spectra

OCP^O was isolated and purified from harvested *Synechocystis* cells by biochemical procedures described in detail in (Boulay et al. 2008; 2010; Stadnichuk et al. 2012). Prior to spectral measurements, to induce the OCP^O → OCP^R phototransformation, the OCP sample was illuminated for 10 min with intense, 1100 $\mu\text{mol photons m}^{-2} \text{s}^{-1}$, blue–green light (tungsten–halogen white light filtered through a 430–540 nm band-pass filter). Absorption spectra of OCP^O (not shown) and OCP^R were recorded using a Hitachi 557 spectrophotometer with a spectral slit width of 2 nm in a 10 mm light-pass cuvette. The absorption spectrum of OCP^R corresponds well to those repeatedly described in the literature.

Rates of energy transfer from PBLcm to PS II and to OCP

Förster resonance energy transfer (FRET) (Förster 1948; Lakowicz 2006; Sener et al. 2011) and excitonic (Agranovich and Galanin 1982; Sener et al. 2011) theories were used to determine the PBS → PS II and PBS → OCP^R energy transfer rates, respectively. Theoretical calculations of energy transfer and quenching were based on the molecular architecture model of the OCP-PBS-PS II supercomplex previously developed in silico from the X-ray crystal structures of APC trimers stacked in cylinders (Zlenko et al. 2017), the PS II dimer (Kern et al. 2005) and the red carotenoid protein (RCP) identical to the N-terminal domain of OCP^R (Leverenz et al. 2015) directly involved in the interaction with PBS. In this model (Krasilnikov et al. 2020), the PBS core was located on the cytoplasmic surface of the PSII dimer together with the RCP globule docked to the collateral region of the PBLcm domain of ApcE, which is part of the basal core cylinder.

Results

Fluorescence emission spectra

The initial steady-state fluorescence emission spectrum of a *Nostoc* sample pre-aged in the dark for 5 min contains the well-known bands of phycobiliproteins and chlorophyll (Fig. 1a). The peak at 574 nm belongs to PE and the band at 660 nm is attributed to bulk APC, while the separate band of PC with the known position at 640 nm is not visible. The separate band at 682 nm of PBLcm is not resolved as it is

superimposed by the most intense band at 685 nm of PS II (Brecht et al. 2014) due to their close superposition. The bright shoulder at about 730 nm is attributed to the sum of long wavelength satellites of the enumerated bands plus some Photosystem I emission.

Under our conditions, the maximum NPQ level was reached within 180 s (3 min) against the background of a slow NPQ process and an even slower reverse process controlled by fluorescence recovery protein (FRP) (Kirilovsky and Kerfeld 2016). This time has been divided into shorter segments to show the successive decrease in intensity of the fluorescence bands. NPQ does not affect PE, as the well-resolved 574 nm peak does not change in height and shape during the whole 180 s and could serve as an additional convenient benchmark to compare the intensity decrease of other bands (Fig. 1A). This result corresponds to the fact that the excitation energy transfer from the PE to the PBS core remains at its maximum level and is therefore not affected by the NPQ, and is consistent with the data that the OCP^R does not come into direct anchoring contact with the lateral cylinders of the PBS (Scott et al. 2006; Stadnichuk et al. 2009; Wilson et al. 2008).

Changes in the amplitude of other fluorescence spectral bands have been observed by tracking the NPQ formation over the first 30 s. The highest degree of quenching was registered for the main fluorescence emission peak around 685 nm. However, as in the original spectrum of the dark-adapted sample (0 s), it was not possible to separate the ApcE (PBLcm) band from the fluorescence superposition with the 685 nm band of PS II in the spectra measured after 30, 60, 120 or 180 s of OCP-dependent phototransformation (Fig. 1a). The resolution of these closely overlapping

spectral bands depends on their relative heights during the quenching process. To reveal the problem in more detail, and to be able to see the NPQ dynamics on the scale of tens of seconds we resort to difference NPQ spectra (Rakhimberdieva et al. 2010) normalized to their peak positions. It was shown that after the first 30 s of high light irradiation, the main peak in the NPQ spectrum shifted from 685 to 682 nm, indicating the presence of the ApcE band (Figure 1b). This is the first direct in vivo evidence that quenching is associated with a change in ApcE fluorescence emission. The much smaller degree of NPQ intensity change in the 660 nm region (Fig. 1b) compared to the 682 and 685 nm bands means that the bulk APC in the PBS core is very unlikely to serve as a site for OCP^R docking in vivo. Again, no bands shorter than 682 nm were observed in these repeated spectral experiments, indicating that ApcD (679 nm) is unlikely to be involved in contact with OCP^R. This result provides additional evidence for the anchoring role of the PBLcm domain of ApcE to previously estimated data (Elanskaya et al. 2018; Stadnichuk et al. 2012; Zhang et al. 2014).

Rate of excitation energy transfer from PBS to PS II

A distance from the nearest phycobilin chromophores within the two basal PBS core cylinders to the antennal chlorophyll molecule(s) of the PS II pigment-protein dimer is estimated to be in the range of 40–48 Å (Chang et al. 2015; Krasilnikov et al. 2020). PBLcm/ApcF-containing APC disk of each basal cylinder is responsible for the protrusion of this disk at the bottom of the PBS core. This protrusion fits well with the hole on the cytoplasmic side of PSII and forms a tight interaction between PBS and PSII (Chang et al. 2015;

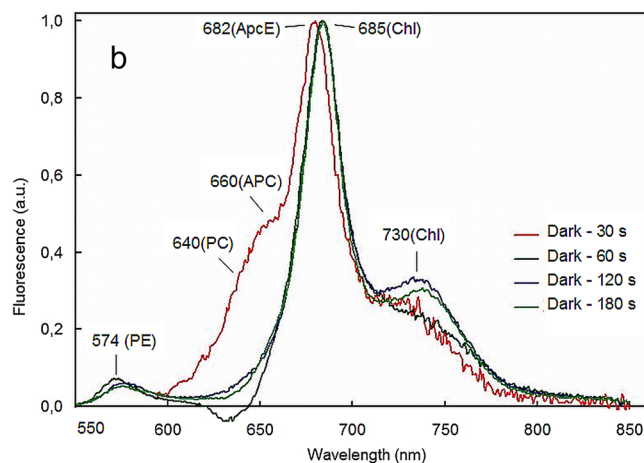
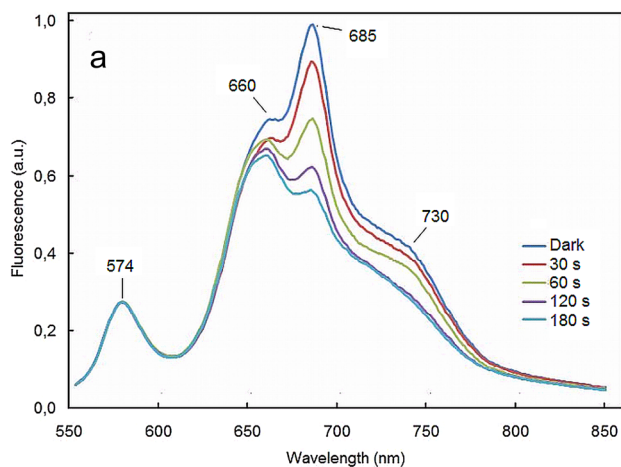


Fig. 1 Fluorescence emission spectra of *Nostoc* cells at room temperature, measured at a series of time points during NPQ development. **a** Spectral changes in OCP-dependent fluorescence intensity at different NPQ times. **b** NPQ spectra obtained as the difference between the dark sample and the same sample for different quenching times. Spec-

tra in **a** and **b** are indicated in the legends on the right with the appropriate color and in **b** spectra are normalized to their main peak positions. The position of the main peak in the “Dark minus 30 s” spectra in five sets of experiments was 682, 682, 682, 682 and 683 nm to 1 nm accuracy

Krasilnikov et al. 2020). Considering the thickness of the apoprotein layer over the near-surface chlorophylls of PS II and the gap created by this protrusion and the amorphous PBLcm loop exposed from the PBS core towards the thylakoid membrane, the distance of 42 Å most likely offered by the model (Krasilnikov et al. 2020) was used here to provide an opportunity for energy transfer from PBS to PS II. The criterion for the sufficiency of the energy transfer only from PBLcm was the agreement of the transfer time determined according to the calculations and established experimentally.

It is implicitly assumed that PBS transfers the absorbed energy to PS II via the FRET mechanism, which is characterized by the notion of the Förster radius (R_0) (Förster 1948; Lakowicz 2006; Kawakami et al. 2022):

$$R_0 = \sqrt[6]{A\Phi_f\chi^2J(\lambda)/n^4} \quad (1)$$

where $A = 9000 \ln 10 / 128 (\pi)^5 N_A \approx 8.8 \cdot 10^{-25}$ mol is a constant. Φ_f is the fluorescence quantum yield of phycocyanobilin chromophores in APC trimers equal to 0.6 (Matamala et al. 2007), $n = 1.33$ is a refractive index of the surrounding medium (Grabowski and Gantt 1978); χ is a factor of the relative orientation of the donor/acceptor dipole transition moments, the overlap integral $J(\lambda)$ is a function of the normalized PBLcm fluorescence emission spectrum, peaked at 682 nm, taken as the donor and the chlorophyll extinction coefficient in PS II as the acceptor. According to the calculations in (Krasilnikov et al. 2020), it is equal to $5.74 \cdot 10^{-13} \text{ cm}^6 \text{ Mol}^{-1}$ for PBLcm/PS II spectral overlap. The transition dipole moments of the PBLcm phycocyanobilin chromophore and the nearest antennal chlorophyll of CP43 appear to be parallel in favorable relative orientation for FRET (Krasilnikov et al. 2020), and thus the orientation factor χ^2 reaches its maximum equal to 4. Based on these values, R_0 was found to be 86 Å. The characteristic time τ of the FRET rate was then calculated as follows:

$$\tau = \tau_d \left(\frac{R}{R_0} \right)^6 \quad (2)$$

where $\tau_d = 1.5\text{--}1.6$ ns (Matamala et al. 2007) is the excited state lifetime of the donor phycocyanobilin chromophore, and R equals 42 Å above. The characteristic time obtained was found to be around 20 ps, which agrees very well with the value determined experimentally for a final step of the PBS → PS II plausible energy transfer pathway (Acuña et al. 2018). According to our present considerations, other phycobilins including the ApcD and ApcF chromophores form an extensive network for energy transfer within the PBS, which routes (Zhao et al. 1992) end in the PBLcm, minimizing direct energy transfer from other phycobilins of the PBS core to PS II. The principles of the PBS core architecture are the same in both the hemidisoidal and bulkier block-type and

hemielipsoidal PBSs of red algae. In particular, the distance between the PBLcm and ApcD chromophores in the PBS cores of the red algae *Griffithsia pacifica* (Zhang et al. 2017), *Porphyridium purpureum* (Ma et al. 2020), the cyanobacteria *Anabaena* 7120, *Synechococcus* 7002 (Zheng et al. 2021) and *Thermosynechococcus vulcanus* (Kawakami et al. 2022) is about 30 Å in all cases determined by cryo-EM microscopy. This implies that the ApcD → PBLcm energy transfer reveals photophysical heterogeneity of PBS transfer pathways (Squires et al. 2019) and must be more efficient than the independent transfer from ApcD to PS II chlorophyll (Krasilnikov et al. 2020).

Excitonic coupling of OCP and PBLcm

The interchromophore distance between the hECN of OCP^R and potential neighboring phycobilin chromophores, due to equally curved lateral surfaces of different APC trimer disks in the PBS core, has to be about 25 Å (Dominguez-Martin et al. 2021; Krasilnikov et al. 2020; Stadnichuk et al. 2015). This conclusion is based on the docking model of APC and OCP crystal structures and the calculated temporal thermodynamic stability of this assembled protein supercomplex (Stadnichuk et al. 2015; Zlenko et al. 2016), as well as the in vitro obtaining of one of the possible complexes of OCP^R and bulk APC as part of the PBS core (Zhang et al. 2014). A priori, the relatively close distance of 25 Å gives reason to consider FRET or excitonic energy transfer (Dominguez-Martin et al. 2021; Krasilnikov et al. 2020; Stadnichuk et al. 2015) from PBS to OCP with subsequent heat dissipation from the ketocarotenoid excited state as the basis for the NPQ mechanism.

The spectral overlap of the $S_0 \rightarrow S_2$ absorption spectrum of OCP^R with the fluorescence emission spectrum of PBLcm was found to be minimal (Fig. 2a), and therefore the time of the estimated FRET calculations in this proposed case should be equal to ~1450 ps (Stadnichuk et al. 2015). A low-lying S_1 state of carotenoids is dipole forbidden for absorption via one-photon transition and is therefore absent from linear absorption spectra measurements (Polivka et al. 1999). The S_1 state energy of hECN with the 0–0 band lying for OCP^R at $14,000 \pm 200 \text{ cm}^{-1}$ (713 nm) has been determined by time-resolved spectroscopy methods (Polivka et al. 2013). Due to a very small value of the $S_0 \rightarrow S_1$ transition density of carotenoids, the extinction coefficient of hECN used for FRET calculations was assumed to be about $1000 \text{ M}^{-1} \text{ cm}^{-1}$ (Stadnichuk et al. 2015); as a result of the strong $1/R^6$ time dependence of the transfer efficiency and the small extinction coefficient, the estimated time of energy migration in this also proposed state should finally be 1650–1700 ps (Stadnichuk et al. 2015). The results of both types of calculations are far from the experimentally determined 20 ps when compared with the step of energy

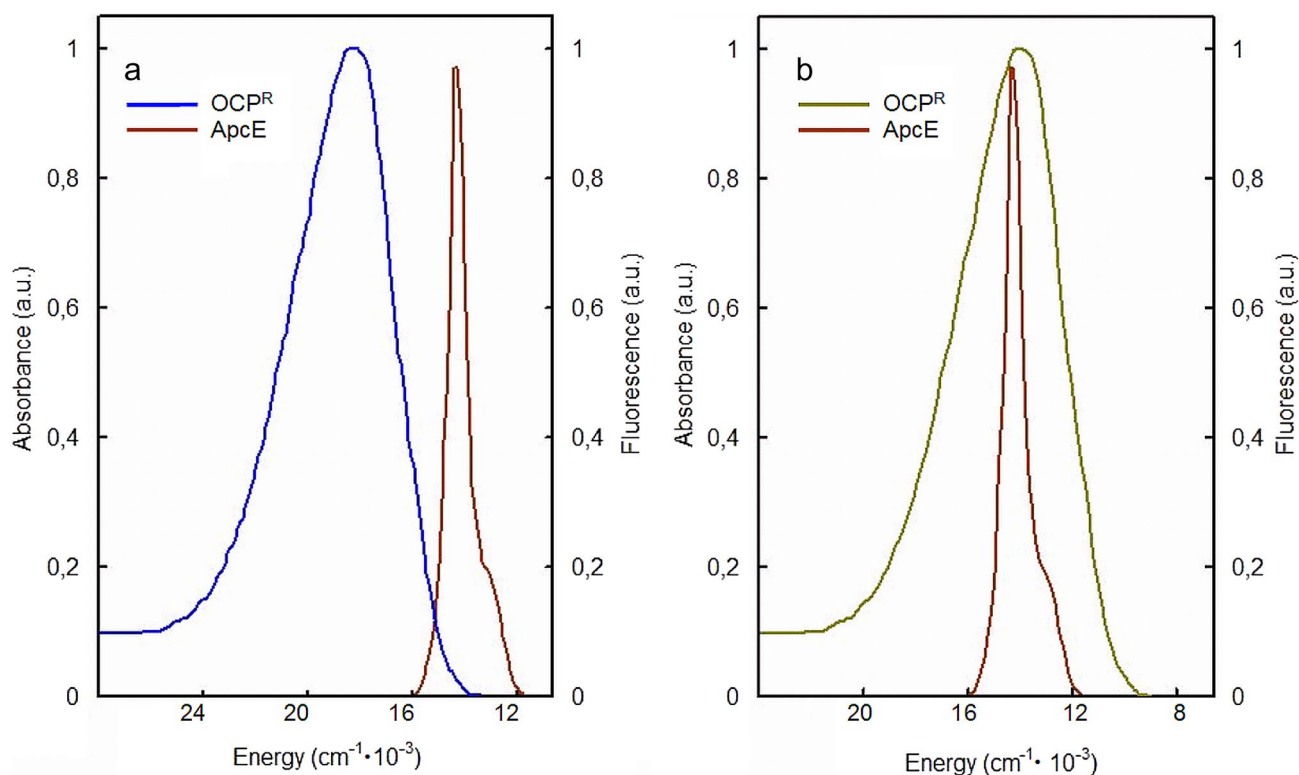


Fig. 2 OCP^R absorption spectra in the S₀→S₂ **a** and S₀→S₁ **b** spectral regions versus fluorescence emission spectrum of PBLcm **a** and **b**. Hypothetical S₀→S₁ absorption spectrum of OCP^R is generated by shifting the experimental S₀→S₂ spectrum to the red region and

using the known specific S₂ and S₁ energy levels for the 0–0 band position of OCP^R. Absorption spectra are overlaid with the emission spectrum for the purpose of demonstration irrelevant spectral overlap in **a** and complete overlap in **b**

migration from PBLcm to PS II (Acuña et al. 2018), and therefore exclude the S₁ and S₂ states of hECN from the OCP^R-dependent energy quenching in the framework of FRET theory.

When the shape of the S₀→S₁ spectrum can be identified for a number of carotenoids (see e.g. Frank et al. 2000), it is seen that it also contains the three main bands typical of carotenoids in non forbidden S₀→S₂ spectra, although with different relative intensities, but in general, an S₀→S₁ spectrum has the same full width on the energy scale as an S₀→S₂ spectrum. In the case of excitonic coupling, the energy resonance, that is the completeness of the overlap between the spectra of two pigments, must be important and their strict contours are irrelevant. For OCP^R, the 0–0 band position of the S₀→S₁ absorption spectrum, determined experimentally by near-infrared femtosecond absorption spectroscopy (Polivka et al. 2013), allows the S₀→S₂ spectrum to be shifted on the energy scale and used to demonstrate the complete overlap of the S₀→S₁ spectrum with the PBLcm fluorescence spectrum due to its large spectral width and despite the likely error in the exact intensity contour. The much broader S₀-S₁ absorption spectrum of OCP^R, constructed by red bathochromic shifting of the known S₀→S₂ transition spectrum to 0–0 band energy value of S₁ compared

to the fluorescence spectrum of PBLcm (peak position at 682 nm corresponds to 14,665 cm⁻¹), here shows such a complete spectral overlap (Fig. 2b). In other words, an absolute prerequisite for excitonic coupling—the complete coincidence of the donor fluorescence and acceptor absorption energy states (Krueger et al. 1998)—is achieved in this case.

The original 3D model of OCP docking to APC in the PBS core (Stadnichuk et al. 2015) was improved (Krasilnikov et al. 2020), to take into account the separation of OCP N- and C-polypeptide domains upon photoactivation of OCP^O (Bondanza et al. 2020; Kerfeld et al. 2017) and the quenching activity of only the N-terminal domain of the formed OCP^R, which is geometrically equivalent to RCP (Lewerenz et al. 2014). The theory of the exciton interaction between the OCP ketocarotenoid and the sterically neighboring phycocyanobilin chromophore of APC was developed and described in detail in (Stadnichuk et al. 2015). The characteristic time τ_q of the excitonic energy transfer from phycocyanobilin of PBLcm to hECN of OCP^R was written as follows (Krasilnikov et al. 2020; Stadnichuk et al. 2015):

$$\tau_q = \frac{\pi \hbar R^3 n^2}{|\chi| \mu_a \mu_d} \quad (3)$$

where according to the geometric model (Krasilnikov et al. 2020), $R = 24.5 \text{ \AA}$ is a distance between the centers of the dipoles of phycobilin and hECN obtained by the docking procedure; $n = 1.33$ is the refractive index (unitless) as in Eq. 1; $\mu_d = 12 \text{ D}$ is the known transition dipole moment of the phycocyanobilin chromophore in Debeyes (Matamala et al. 2007; Ren et al. 2013) and $\mu_a = 1.8 \text{ D}$ was previously obtained from quantum chemical calculation of the virtual $S_0 \rightarrow S_1$ transition dipole moment of hECN in OCP^R (Stadnichuk et al. 2015).

In the combined tripartite RCP-PBLcm-PS II model created (Krasilnikov et al. 2020), the main condition was considered above the plausible energy transfer from PBS to PS II. The transition dipole moment of phycocyanobilin of PBLcm in the model is optimally directed for photosynthetic energy transfer ($|\chi| = 2$) to the nearest chlorophyll of PS II (#47 of CP43) (Loll et al. 2005). Relatedly, the direction of the hECN transient dipole moment vector is secondary. The combined geometric positions of the PBLcm-PSII and PBLcm-RCP pairs then only allow the placement of the RCP such that the carotenoid hECN molecule would be nearly perpendicular to the axis of the PBS core cylinders. Any other orientation of the RCP with the $S_0 \rightarrow S_1$ transition dipole moment of hECN directed along the conjugated chain of the hECN carotenoid molecule (Hashimoto et al. 2018) is limited by the strong steric clashes. As a result, the orientation factor $|\chi|$ between the transition dipole moments of hECN and the chromophore of PBLcm appeared to be small, only 0.24–0.42. The duration of energy transfer time and quenching by the excitonic mechanism is inversely proportional to the values of the orientation factor and the transition dipole moments of the interacting chromophores (Eq. 3). Despite the unfavorable low value of the factor $|\chi|$, the probable characteristic time obtained here was in the range of 1.5–2.6 ps, which cannot yet be more precisely determined. The larger time previously calculated in (Stadnichuk et al. 2015) did not exceed 10 ps. Nevertheless, the obtained values of the characteristic time were two orders of magnitude smaller than purely speculative for the OCP^R calculations within FRET theory and 2–5 times smaller than the final step time of energy migration from PBLcm to PS II (Acuña et al. 2018).

Discussion

Possible mechanisms of carotenoid-induced quenching

Several models explaining the direct involvement of carotenoids in NPQ currently exist. (1) FRET between the quenched pigment molecule and the carotenoid (Staleva et al. 2015). (2) Charge transfer between these two molecules in close proximity (Holt et al. 2005). (3) Potential

involvement in energy transfer of specific ICT state formed in OCP and some other carotenoids (Šlouf et al. 2017). (4) Excitonic coupling of two such molecules, involving dipole–dipole and possibly dipole–quadrupole interactions. Our calculations, presented in this paper and previously in more detail (Stadnichuk et al. 2015), show that the proposed FRET from ApcE to the OCP carotenoid requires not less than 1000 ps. Because it's slow compared to transferring energy from PBS to PS II, this means that the S2 or S1 energy levels of the OCP carotenoid could not be sufficiently populated. Electron transfer, which could be associated with quenching, as we understand it, shows no evidence of the OCP carotenoid anion. Such a mechanism is unlikely as, to our knowledge, there is also no clear data on phycocyanobilin cation formation in the literature.

The spectrum of the OCP carotenoid after light absorption and relaxation from the S2 state is more complex, as it may contain an additional redshifted band, usually attributed to a transition from the intramolecular charge transfer (ICT) state. Investigation of this issue using examples of structurally similar carotenoids, but with or without a pronounced ICT state, has shown that the presence of the ICT moiety in the OCP carotenoid is unlikely to play a role in quenching (Šlouf et al. 2017). The exciton mechanism of the dipole–quadrupole interaction can, in principle, be realized in quenching process too. However, the quadrupole–dipole interaction is not dominant as its intensity is at least one order of magnitude smaller than that of the dipole–dipole interaction. The quadrupole moment is taken into account when the dipole moment is very small (Agranovich and Galanin 1982). When the dipole–dipole interaction is non-zero, as in the case of OCP^R and PBLcm chromophores, the quadrupole–dipole interaction is negligible here. Furthermore, the quadrupole–dipole interaction decreases more with distance ($\sim R^{-5}$). This can be relevant when two neighboring pigment molecules are very close together, as in the case of a number of photosynthetic antennae containing chlorophylls or bacteriochlorophylls belonging to the same apoprotein. OCP^R and PBLcm are two different proteins of cyanobacteria where the interchromophore distance is 25.5 Å in the quenching state of PBS and the quadrupole role can be ignored. The likelihood of a dipole–dipole interaction between the ApcE and OCP chromophores during quenching seems to be increased by these brief arguments. Given the existence of other NPQ hypotheses, the question is open for further experiments and discussion.

PBS to OCP ratio and the rate of NPQ in vivo

NPQ in cyanobacteria can be defined as a decrease in the fluorescence intensity of PBSs and consequently chlorophyll resulting in reduced energy supply to PS II from quenched

PBSs due to OCP photoactivation. Each PBS in thylakoids is considered to be a discrete protein macrocomplex that can interact with OCP^R independently of other PBSs under high light conditions. (We do not consider the case of potential PBS rows formation during State 1/State 2 transitions (Zlenko et al. 2017). The ratio of OCP to PBS in cyanobacterial cells is known to be 1:2 (Wilson et al. 2008). That's for even after complete photoactivation of all cellular OCP molecules and full NPQ development half of the cellular PBSs remain OCP^R-free and fully retain their original ability to transfer energy to PS II. Quenching efficiency based on this ratio and the ratio of quenching and energy transfer to PS II characteristic times (~2 ps: 20 ps) cannot exceed 50%. This estimate is supported by experimental data that OCP-dependent quenching affects only about half of the PBSs coupled to PS II (Protasova et al. 2021) and does not exceed 40–45% (Kerfeld et al. 2017; Rakhimberdieva et al. 2004, 2010). For the fraction of PBS associated with the OCP^R, it can be assumed, without loss of generality, that each PBS interacts with one OCP^R molecule. This means that, on average, one of the two PBLcm located in the two basal cylinders of the PBS core remains unconnected to the OCP^R. Assuming that, due to bilateral symmetry, the energy transfer flows within each PBS terminate equally at the two PBLcm, the fluorescence of such PBS, “half OCP^R supplied”, can also only be reduced by 50%, since the second PBLcm remains free of OCP^R. Taken together, on average, three out of each four PBLcm in cellular PBSs are not involved in interaction with the OCP^R. PBS fluorescence in the cell can be quenched only by 25% in such an estimate, whereas the experimental value is almost twice as high (Kerfeld et al. 2017; Rakhimberdieva et al. 2004; 2010). Thus, theoretical estimation leads to a contradiction, with actual quenching higher than such reasoning would suggest.

We speculate that the experimental 40–45% quenching rate achieved after docking in average of a single OCP^R molecules to only half of the PBSs from their cell population, is the result of an additional redistribution of energy flow within the PBS phycobilins and the PBLcm chromophore free of interaction with the OCP^R in favor of the second PBLcm with docked OCP^R (Fig. 3). In this respect, it should be noted that the two ApcFs are located in the same APC trimers as the PBLcm and, in their auxiliary functions, can serve to bridge the lateral transfer of energy between the cylinders of the PBS core. The large difference in the OCP^R-induced quenching time, which does not exceed 1.5–2.5 ps, and the 20 ps time of the energy transfer step from PBLcm to PS II, provokes the redistribution of energy flows. This conclusion is consistent with data on positional switching of PBS core cylinders and increased conformational mobility of phycocyanobilin chromophores as a function of heat and light induced PBS reorganizations (Stoitchkova et al. 2007) and OCP binding (Dominguez-Martin et al.

2021). Due to the presence of several hundred phycobilin chromophores in hemidiscoidal cyanobacterial PBS (Adir et al. 2019; Chang et al. 2015; Sidler 1994) and several internal PBS energy transfer pathways to PBLcm (Zheng et al. 2021), the quantitative calculation of the corresponding changes in migration pathways within PBS upon attachment of OCP^R cannot be convincing enough. The possibility of switching of energy transfer pathways within PBS may explain the efficient use of the fast OCP^R-dependent exciton mechanism of quenching, which proves effective despite the lower number of OCP^R molecules in the cell compared to PBS.

Similarities and differences between the NPQ process in solution and in the cyanobacterial cell

It is well established that PBSs are located on the surface of the PS II dimers with their two core basal cylinders in the plane of the thylakoid membrane (Adir et al. 2019; Arteni et al. 2009; Bald et al. 1996; Bryant and Canniffe 2018). Several details of the possible relative positions of the PBS and PS II dimer with their twofold symmetry have been revealed by cryo-EM and cross-linking/mass spectrometry techniques (Arteni et al. 2009; Chang et al. 2015). To date, a reliable way to study the formation of water-soluble PBS and membranous PS II supercomplexes remains the use of spatial computer modeling based on the known crystallographic and EM data (Bryant and Canniffe 2018; Chang et al. 2015; Zlenko et al. 2017).

Depending on the light intensity, the total NPQ implementation time in cyanobacterial cells is typically a few minutes (Rakhimberdieva et al. 2004; Wilson et al. 2006). PAM fluorometry and/or steady-state fluorescence spectra measured at the end of the quenching process do not reveal subtle acquisition spectral changes during NPQ evolution. Time-resolved spectrofluorimetry requires prior mathematical modeling and therefore has some shortcomings. We have taken advantage of tracking changes in the emitted fluorescence spectra of *Nostoc* over tens of seconds.

Our findings are based on the established leading role of PBLcm in reducing fluorescence during NPQ development in vivo (Fig. 1) and supported by the calculated exciton interaction at S₁ energy levels of the phycobilin chromophore in PBLcm and the hECN carotenoid in OCP^R. PBLcm thus acts as a splitting point for the energy delivered by the phycobilisomal antenna to PS II, to intercept it and carry out the quenching process. Due to OCP, cyanobacterial PBSs have a special type of NPQ among antenna complexes (Arshad et al. 2022). The water solubility of OCP and PBS makes it possible to study the phenomenon of NPQ in solution, transferring the established regularities to the process of quenching in the cyanobacterial cell. These data lead to the question of the similarities

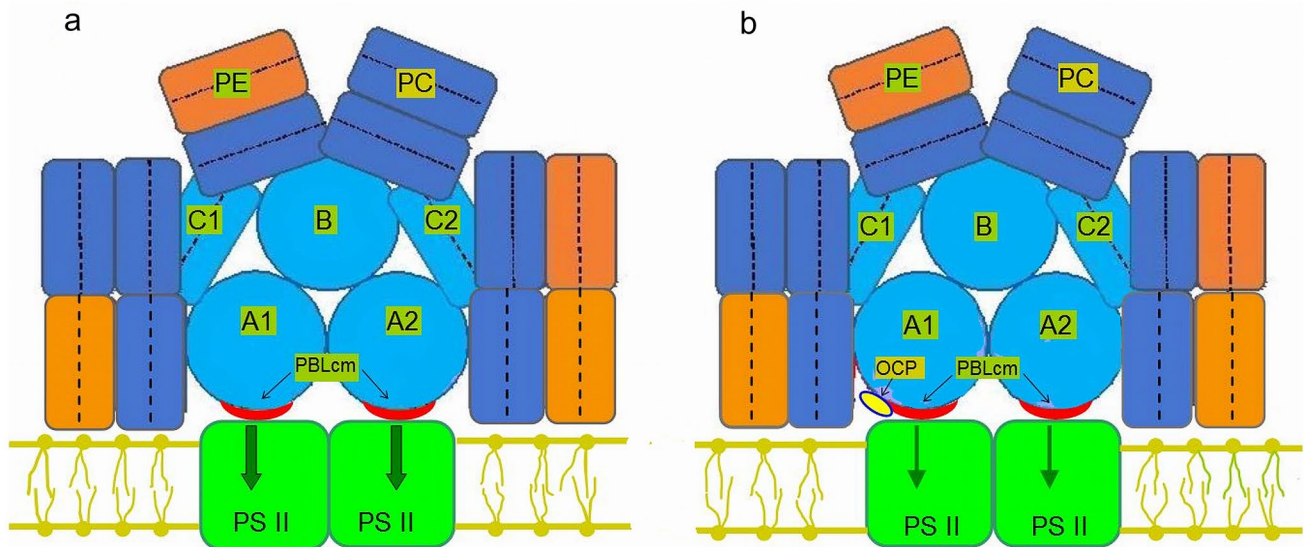


Fig. 3 Schematic views of the PBS-PSII supercomplex in *Nostoc* thylakoids without **a** and with **b** OCP^R attached to one of the two PBLcm domains in PBS core. Phycoerythrin and phycocyanin of the lateral cylinders and allophycocyanin of the pentacylindrical PBS core are denoted PE, PC and APC, as in the text. They are shown in orange, blue and sky blue, respectively. The two lower APC cylinders of the core are designated as A1 and A2, the central cylinder as B, and the two upper cylinders as C1 and C2, in accordance with the

nomenclature of Chang et al. 2015. The parts of the two PBLcm protruding from the PBS to the thylakoid membrane in the bottom core cylinders are shown as red arcs; the OCP^R attached to one of the two PBLcm is shown as a yellow oval. The PS II dimers are shown in light green, with arrows indicating the direction of energy flow from the PBLcm to the antennal chlorophyll of PS II. A decrease in the thickness of the arrows **b** indicates a decrease in the level of energy transfer from PBLcm to PS II during the time of OCP^R attachment

and differences between the course of NPQ in vivo and in vitro. The direct contact between OCP and PBS is the main common pattern for NPQ in cell and solution. (Gwizdala et al. 2011; Stadnichuk et al. 2011). The photophysical and photochemical properties of OCP studied, including the OCP^O → OCP^R transformation under high light conditions, the presence of transformed N- and C-domains within the OCP molecule and the role of each domain in the development of quenching, as well as many other properties of OCP, are common to cyanobacterial cells and to modeling in solution (Gwizdala et al. 2011; Stadnichuk et al. 2011). Besides the similarities, there are also differences, which are summed up by Table 1 and can be discussed against the background of the results presented here.

Based on numerous studies of the NPQ effect and the properties of OCP in cyanobacteria and in solution: Acuña et al. 2018; Boulay et al. 2008; Dominguez-Martin et al. 2021; Elanskaya et al. 2018; Grabowski and Gantt 1978; Gwizdala et al. 2011; Kerfeld et al. 2017; Kirilovsky and Kerfeld 2016; Lewerenz et al. 2014; Maksimov et al. 2014; Matamala et al. 2007; Rakhimberdieva et al. 2010; Stadnichuk et al. 2011; Tian et al. 2011; Wilson et al. 2006; Zlenko et al. 2019. (Some features present in the table such as type of quenching and reverse energy flow in PBS are not mentioned and analyzed in the text).

The most striking difference is the fact that almost 100% PBS quenching can be achieved in vitro (Kerfeld et al. 2017). However, for such an effect, the amount of OCP^R in solution must be several tens of times the amount of PBS (Table 1). In solution, the likelihood of OCP interacting with PBS due to the diffusion process is dramatically reduced and compensated for by a high OCP content and the possibility of additional surface contacts of OCP with the bulk APC trimers. In the cyanobacterial cell, the efficiency of the much lower OCP^R/PBS ratio is ensured by the localization of OCP in close proximity to the loop insertion, which is part of the PBLcm domain and appears to provide an optimal position for OCP to implement NPQ (Zlenko et al. 2019). PS II complexes are absent from in vitro OCP and PBS interaction experiments due to their insolubility in aqueous solutions. Accordingly, the energy transfer channel from PBS to PS II is absent and the lifetime of the excited state of the phycobilin chromophores in PBS increases significantly (Grabowski and Gantt 1978; Matamala et al. 2007). According to (Dominguez-Martin et al. 2021), this fact, together with the exciton interaction of OCP with the PBLcm chromophore, suggests that the possibility of energy transfer via the FRET mechanism from the phycobilins of the bulk APC trimers of PBS to the abundance of OCP molecules present in solution could also be substantially increased. It is also important that NPQ must be reversible in the cell with cycles of photoactivation and dark deactivation of OCP molecules due to the

Table 1 Main properties of NPQ in vivo and in vitro

Nº	NPQ characteristics	In vivo	In vitro
1	Quenching efficiency	40–45%	90–95%
2	OCP/PBS ratio	1 OCP molecule per 2–3 PBSs	20–40 OCP molecules per 1 PBS
3	Site(s) of OCP docking to PBS	PBLcm domain of ApcE	Bulk APC and PBLcm domain of ApcE
4	Type of quenching	Specific (dynamic)	Specific and non-specific (dynamic and static)
5	Placement of OCP	In thin cytoplasmic layer close to thylakoid surface	Diffuse placement throughout solution volume
6	Availability of PBS surface to OCP	Availability is limited to PBS surface not involved in placement on the thylakoid membrane	All PBS surface is available
7	Proportion of quenched PBSs	On average, 50% of PBSs remain unquenched due to lack of OCP molecules	All PBSs in solution are available for quenching
8	Direction of energy flow in PBS core	Effective direct energy flow from PBS to chlorophyll minimizes reverse energy transfer between PBS chromophores	Presence of direct and reverse energy flow from bulk APC to PBLcm
9	Lifetime of excitation in PBS	Average, 200 ps energy transfer time from PBS chromophores to PBLcm and 20 ps time for the final migration step from PBLcm to PS II	Intrinsic lifetime of excitation in PBS is equal to 1600 ps

presence of FRP, which ensures the repeated participation of OCP in the acts of implementing the effect, but this issue is beyond the FRP-driven molecular mechanism (Boulay et al. 2010; Kerfeld et al. 2017).

Author contributions PMK and INS designed the project. INS performed the fluorescence spectra measurements and wrote the manuscript. PMK performed the energy transfer calculations and evaluated the results.

Funding The research was carried out within the state assignment of the Ministry of Science and Higher Education of the Russian Federation (Theme No 122042700044-6).

Data availability References to the statement that data are available are included.

Declarations

Competing interests The authors have no relevant financial or non-financial interests to disclose.

Ethical approval Not applicable.

Informed consent Not applicable.

Research involving human and animal rights Not applicable.

References

- Acuña AM, van Alphen P, van Grondelle R, van Stokkum IHM (2018) The phycobilisome terminal emitter transfers its energy with a rate of $(20\text{ps})^{-1}$ to photosystem II. *Photosynthetica* 56:265–274. <https://doi.org/10.1007/s11099-018-0779-7>
- Adir N, Bar-Zvi S, Harris D (2019) The amazing phycobilisome. *Biochim Biophys Acta*. <https://doi.org/10.1016/j.bbabi.2019.07.002>
- Agranovich VM, Galanin MD (1982) Electronic excitation energy transfer in condensed matter. North-Holland Publishing Co, Amsterdam
- Arshad R, Saccon F, Bag P, Biswas A, Calvaruso C, Bhatti AF, Grebe S, Mascoli V, Mahub M, Muzzopappa F, Polyzois A, Schiphorst C, Sorrentino M, Streckaite S, van Amerongen H, Aro E-M, Bassi R, Boekema EJ, Croce R, Dekker J, van Grondelle R, Jansson S, Kirilovsky D, Kouril R, Michel S, Mullineaux CW, Panzarova K, Robert B, Ruban AV, van Stokkum I, Wientjes E, Büchel C (2022) A kaleidoscope of photosynthetic antenna proteins and their emerging roles. *Plant Physiol* 189:1204–1219. <https://doi.org/10.1093/plphys/kiac175>
- Arteni AA, Ajlani G, Boekema EJ (2009) Structural organization of phycobilisomes from *Synechocystis* strain PCC 6803 and their interaction with the membrane. *Biochim Biophys Acta* 1787:272–279. <https://doi.org/10.1016/j.bbabi.2009.01.009>
- Bald D, Kruip J, Rögner M (1996) Supramolecular architecture of cyanobacterial thylakoid membranes: How is the phycobilisome connected with the photosystems? *Photosynth Res* 49:103–118. <https://doi.org/10.1007/BF00117661>
- Bernát G, Schreiber U, Sendtko E, Stadnichuk IN, Rexroth S, Rögner M, Koenig F (2012) Unique properties vs. common themes: The atypical cyanobacterium *Gloeobacter violaceus* PCC 7421 is capable of state transitions and blue-light-induced fluorescence quenching. *Plant Cell Physiol* 53:528–542. <https://doi.org/10.1093/pcp/pcs009>
- Bondanza M, Cupellini L, Lippardini F, Mennucci B (2020) The multiple roles of the protein in the photoactivation of orange carotenoid protein. *Chem* 6:187–203. <https://doi.org/10.1016/j.chempr.2019.10.014>
- Boulay C, Abasova L, Six C, Vass I, Kirilovsky D (2008) Occurrence and function of the orange carotenoid protein in photoprotective mechanisms in various cyanobacteria. *Biochim Biophys Acta* 1777:1344–1354. <https://doi.org/10.1016/j.bbabi.2008.07.002>
- Boulay C, Wilson A, D'Haene S, Kirilovsky D (2010) Identification of a protein required for recovery of full antenna capacity in OCP-related photoprotective mechanism in cyanobacteria. *Proc Natl Acad Sci USA* 107:11620–11625. <https://doi.org/10.1073/pnas.1002912107>

- Brecht M, Skandary S, Hellmich J, Glöckner C, Konrad A, Hussels M, Meixner AJ, Zouni A, Schlodder E (2014) Spectroscopic properties of photosystem II core complexes from *Thermosynechococcus elongatus* revealed by single-molecule experiments. *Biochim Biophys Acta-Bioenergetics* 1837:773–781. <https://doi.org/10.1016/j.bbabi.2014.01.025>
- Bryant DA, Canniffe DP (2018) How nature designs light-harvesting antenna systems: design principles and functional realization in chlorophototrophic prokaryotes. *J Phys B at Mol Opt Phys*. <https://doi.org/10.1088/1361-6455/aa9c3c>
- Calzadilla PI, Kirilovsky D (2020) Revisiting cyanobacterial state transitions. *Photochem Photobiol Sci* 19:585. <https://doi.org/10.1039/c9pp00451c>
- Calzadilla PI, Muzzopappa F, Sétif P, Kirilovsky D (2019) Different roles for ApcD and ApcF in *Synechococcus elongatus* and *Synechocystis* sp. PCC 6803 phycobilisomes. *Biochim Biophys Acta-Bioenerg* 1860:488–498. <https://doi.org/10.1016/j.bbabi.2019.04.004>
- Capuano V, Braux AS, deMarsac NT, Houmard J (1991) The “anchor polypeptide” of cyanobacterial phycobilisomes. Molecular characterization of the *Synechococcus* sp. PCC 6301 *apcE* gene. *J Biol Chem* 266:7239–7247. [https://doi.org/10.1016/S0021-9258\(20\)89636-7](https://doi.org/10.1016/S0021-9258(20)89636-7)
- Chang L, Liu X, Li Y, Liu CC, Yang F, Zhao J, Sui SF (2015) Structural organization of an intact phycobilisome and its association with photosystem II. *Cell Res* 25:726–737. <https://doi.org/10.1038/cr.2015.59>
- Domínguez-Martin MA, Sauer PV, Sutter M, Kirst H, Bina D, Greber BJ, Nogales E, Polívka T, Kerfeld CA (2021) Structure of the quenched cyanobacterial OCP-phycobilisome complex. *BioRxiv*. <https://doi.org/10.1101/2021.11.15.468719>
- Domínguez-Martin MA, Sauer PV, Kirst H, Sutter M, Bina D, Greber BJ, Nogales E, Polívka T, Kerfeld CA (2022) Structures of a phycobilisome in light-harvesting and photoprotected states. *Nature* 609:835–845. <https://doi.org/10.1038/s41586-022-05156-4>
- Dong C, Tang A, Zhao J, Mullineaux CW, Shen G, Bryant DA (2009) ApcD is necessary for efficient energy transfer from phycobilisomes to photosystem I and helps to prevent photoinhibition in the cyanobacterium *Synechococcus* sp. PCC 7002. *Biochim Biophys Acta* 1787:1122–1128. <https://doi.org/10.1016/j.bbabi.2009.04.007>
- Elanskaya IV, Zlenko DV, Lukashev EP, Suzina NE, Kononova IA, Stadnichuk IN (2018) Phycobilisomes from the mutant cyanobacterium *Synechocystis* sp. PCC 6803 missing chromophore domain of ApcE. *Biochim Biophys Acta Bioenergetics* 1859:280–291. <https://doi.org/10.1016/j.bbabi.2018.01.003>
- Förster T (1948) Zwischenmolekulare Energiewanderung und Fluoreszenz. *Ann Phys* 437:55–75
- Frank HA, Bautista JA, Josue JS, Young AJ (2000) Mechanism of non-photochemical quenching in green plants: energies of the lowest excited singlet states of violaxanthin and zeaxanthin. *Biochemistry* 39:2831–2837. <https://doi.org/10.1021/bi9924664>
- Gindt YM, Zhou J, Bryant D, Sauer K (1994) Spectroscopic studies of phycobilisome subcore preparations lacking key core chromophores: assignment of excited state energies to the L_{CM}, β¹⁸ and α chromophores. *Biochim Biophys Acta* 1186:153–162. [https://doi.org/10.1016/0005-2728\(94\)90174-0](https://doi.org/10.1016/0005-2728(94)90174-0)
- Glazer AN (1994) Adaptive variations in phycobilisome structure. *Adv Mol Cell Biol* 10:119–149
- Grabowski B, Gantt E (1978) Excitation energy migration in phycobilisomes: comparison of experimental results and theoretical predictions. *Photochem Photobiol* 28:47–54. <https://doi.org/10.1111/j.1751-1097.1978.tb06928.x>
- Gwizdala M, Wilson A, Kirilovsky D (2011) In vitro reconstitution of the cyanobacterial photoprotective mechanism mediated by the orange carotenoid protein in *Synechocystis* PCC 6803. *Plant Cell* 23:2631–2643. <https://doi.org/10.1105/tpc.111.086884>
- Hashimoto H, Urugami C, Yukihiro N, Gardiner AT, Cogdell RJ (2018) Understanding/unravelling carotenoid excited singlet states. *J R Soc, Interface* 15:20180026. <https://doi.org/10.1098/rsif.2018.00267>
- Hirose Y, Narikawa R, Katayama M, Ikeuchi M (2010) Cyanobacteriochrome CcaS regulates phycoerythrin accumulation in *Nostoc punctiforme*, a group II chromatic adapter. *Proc Natl Acad Sci USA* 107:8854–8859. <https://doi.org/10.1073/pnas.1000177107>
- Holt NE, Zigmantas D, Valkunas L et al (2005) Carotenoid cation formation and the regulation of photosynthetic light harvesting. *Science* 307:433–436. <https://doi.org/10.1126/science.1105833>
- Kawakami K, Hamaguchi T, Hirose Y, Kosumi D, Miyata M, Kamiya N, Yonekura K (2022) Core and rod structures of a thermophilic cyanobacterial light-harvesting phycobilisome. *Nat Commun* 17:3389. <https://doi.org/10.1038/s41467-022-30962-9>
- Kerfeld CA, Melnicki MR, Sutter M, Dominguez-Martin MA (2017) Structure, function and evolution of the cyanobacterial orange carotenoid protein and its homologs. *New Phytol* 215:937–951. <https://doi.org/10.1111/nph.14670>
- Kern J, Loll B, Lüneberg C, DiFiore D, Biesiadka J, Irrgang K-D, Zouni A (2005) Purification, characterisation and crystallisation of photosystem II from *Thermosynechococcus elongatus* cultivated in a new type of photobioreactor. *Biochim Biophys Acta* 1706:147–157. <https://doi.org/10.1016/j.bbabi.2004.10.007>
- Kirilovsky D, Kerfeld CA (2016) Cyanobacterial photoprotection by the orange carotenoid protein. *Nature Plants* 2:16180. <https://doi.org/10.1038/nplants.2016.180>
- Krasilnikov PM, Zlenko DV, Stadnichuk IN (2020) Rates and pathways of energy migration from the phycobilisome to the photosystem II and to the orange carotenoid protein in cyanobacteria. *FEBS Lett* 594:1145–1154. <https://doi.org/10.1002/1873-3468.13709>
- Krueger BP, Scholes GD, Fleming GR (1998) Calculation of couplings and energy-transfer pathways between the pigments of LH2 by the ab initio transition density cube method. *J Phys Chem B* 102:5378–5386. <https://doi.org/10.1021/jp973062t>
- Lakowicz JR (2006) Principles of fluorescence spectroscopy. Springer, New York
- Leverenz RL, Jallet D, Li MD, Mathies RA, Kirilovsky D, Kerfeld CA (2014) Structural and functional modularity of the orange carotenoid protein: distinct roles for the N- and C-terminal domains in cyanobacterial photoprotection. *Plant Cell* 26:426–437. <https://doi.org/10.1105/tpc.113.118588>
- Leverenz RL, Sutter M, Wilson A, Gupta S, Thurotte A, Bourcier de Carbon C, Petzold CJ, Ralston C, Perreau F, Kirilovsky D, Kerfeld CA (2015) A 12 Å carotenoid translocation in a photo-switch associated with cyanobacterial photoprotection. *Science* 348:1463–1466. <https://doi.org/10.1126/science.aaa7234>
- Liu N, Chen XL, Zhang Y-Z, Zhou BC (2005) Characterization, structure and function of linker polypeptides in phycobilisomes of cyanobacteria and red algae: an overview. *Biochim Biophys Acta* 1708:133–142. <https://doi.org/10.1016/j.bbabi.2005.04.001>
- Liu H, Zhang H, Niedzwiedzki DM, Prado M, He G, Gross ML et al (2013) Phycobilisomes supply excitations to both photosystems in a megacomplex in cyanobacteria. *Science* 342:1104–1107. <https://doi.org/10.1126/science.1242321>
- Loll B, Kern J, Saenger WZ, A, Biesiadka J, (2005) Towards complete cofactor arrangement in the 3.0 Å resolution structure of photosystem II. *Nature* 438:1040–1044. <https://doi.org/10.1038/nature04224>
- Lundell DJ, Glazer AN (1981) Allophycocyanin B. A common β-subunit in *Synechococcus* allophycocyanin B (λ_{max} 670 nm) and allophycocyanin (λ_{max} 650 nm). *J Biol Chem* 256:12600–12606. [https://doi.org/10.1016/S0021-9258\(18\)43317-0](https://doi.org/10.1016/S0021-9258(18)43317-0)

- Ma J, You X, Sun S, Wang X, Qin S, Sui SF (2020) Structural basis of energy transfer in *Porphyridium purpureum* phycobilisome. *Nature* 579:146–151. <https://doi.org/10.1038/nature24278>
- Maksimov E, Schmitt F, Shirshin E, Svirin M, Elanskaya I, Friedrich T, Fadeev V, Paschenko V, Rubin A (2014) The time course of non-photochemical quenching in phycobilisomes of *Synechocystis* sp. PCC 6803 as revealed by picosecond timeresolved fluorimetry. *Biochim Biophys Acta* 1837:1540–1547. <https://doi.org/10.1016/j.bbabi.2014.01.010>
- Manodori A, Alhadef M, Glazer AN, Melis A (1985) Phycobilisome-photosystem II association in *Synechococcus* 6301 (Cyanophyceae). *FEBS Lett* 181:79–82
- Matamala AR, Almonacid DE, Figueroa MF, Martinez-Oyanedel J, Bunster MC (2007) A semiempirical approach to the intra-phycocyanin and inter-phycocyanin fluorescence resonance energy transfer pathways in phycobilisomes. *J Comput Chem* 28:1200–1207. <https://doi.org/10.1002/jcc.20634>
- Meeks JC, Elhai J, Thiel T, Potts M, Larimer F, Lamerdin J, Predk P, Atlas R (2001) An overview of the genome of *Nostoc punctiforme*, a multicellular, symbiotic cyanobacterium. *Photosynth Res* 70:85–106. <https://doi.org/10.1023/A:1013840025518>
- Mimuro M, Gantt E (1986) A high molecular weight terminal pigment ('anchor polypeptide') and a minor blue polypeptide from phycobilisomes of the cyanobacterium *Nostoc* sp. (MAC): isolation and characterization. *Photosynth Res* 10:201–208. <https://doi.org/10.1007/BF00118284>
- Mimuro M, Lipschultz C, Gantt E (1986) Energy flow in the phycobilisome core of *Nostoc* sp. (MAC): two independent terminal pigments. *Biochim Biophys Acta-Bioenergetics* 852:126–132. [https://doi.org/10.1016/0005-2728\(86\)90065-4](https://doi.org/10.1016/0005-2728(86)90065-4)
- Mullineaux CW (1994) Excitation energy transfer from phycobilisomes to photosystem I in cyanobacterial mutant lacking photosystem II. *Biochim Biophys Acta* 1184:71–77. [https://doi.org/10.1016/0005-2728\(94\)90155-4](https://doi.org/10.1016/0005-2728(94)90155-4)
- Polívka T, Herek JL, Zigmantas D, Akerlund H-S (1999) Direct observation of the (forbidden) S₁ state in carotenoids *Proc Natl Acad Sci USA* 96:4914–4917. <https://doi.org/10.1073/pnas.96.9.4914>
- Polívka T, Chábera P, Kerfeld CA (2013) Carotenoid–protein interaction alters the S₁ energy of hydroxyechinenone in the orange carotenoid protein. *Biochim Biophys Acta* 1827:248–254. <https://doi.org/10.1016/j.bbabi.2012.10.005>
- Protasova EA, Antal TK, Zlenko DV, Elanskaya IV, Lukashev EP, Friedrich T, Mironov KS, Sluchanko NN, Ge B, Qin S, Maksimov EG (2021) State of the phycobilisome determines effective absorption cross-section of photosystem II in *Synechocystis* sp. PCC 6803. *Biochim Biophys Acta-Bioenerg*. <https://doi.org/10.1016/j.bbabi.2021.148494>
- Rakhimberdieva MG, Stadnichuk IN, Elanskaya IV, Karapetyan NV (2004) Carotenoid induced quenching of the phycobilisome fluorescence in photosystem II-deficient mutant of *Synechocystis* sp. PCC 6803. *FEBS Lett* 574:85–88. <https://doi.org/10.1016/j.febslet.2004.07.087>
- Rakhimberdieva MG, Elanskaya IV, Vermaas W, Karapetyan NV (2010) Carotenoid triggered energy dissipation in phycobilisomes of *Synechocystis* sp. PCC 6803 diverts excitation away from reaction centers of both photosystems. *Biochim Biophys Acta* 1797:241–249. <https://doi.org/10.1016/j.bbabi.2009.10.008>
- Ren Y, Chi B, Melhem O, Wei K, Feng L, Li Y, Han X, Li D, Zhang Y, Wan J, Xu X, Yang M (2013) Understanding the electronic energy transfer pathways in the trimeric and hexameric aggregation state of cyanobacterial phycocyanin within the framework of Förster theory. *J Comp Chem* 34:1005–1012. <https://doi.org/10.1002/jcc.23221>
- Scott M, McCollum C, Vasil'ev S, Crozier C, Espie GS, Krol M, Huner NPA, Bruce D C (2006) Mechanism of the down regulation of photosynthesis by blue light in the cyanobacterium *Synechocystis* sp. PCC 6803. *Biochemistry* 45:8952–8958. <https://doi.org/10.1021/bi060767p>
- Sener M, Strümpfer J, Hsin J, Chandler D, Scheuring S, Hunter CN, Schulten K (2011) Förster energy transfer theory as reflected in the structures of photosynthetic light-harvesting systems. *ChemPhysChem* 12:518–531. <https://doi.org/10.1002/cphc.201000944>
- Sidler WA (1994) Phycobilisome and phycobiliprotein structures. In: Bryant DA (ed) *The Molecular Biology of Cyanobacteria*. Springer, Dordrecht, pp 139–216
- Šlouf V, Kuznetsova V, Fuciman M, Bourcier de Carbon C, Wilson A, Kirilovsky D, Polívka T, Jallet D, Gwizdala M, Kirilovsky D (2012) ApcD, ApcF and ApcE are not required for the orange carotenoid protein related phycobilisome fluorescence quenching in the cyanobacterium *Synechocystis* PCC 6803. *Biochim Biophys Acta* 1817:1418–1427. <https://doi.org/10.1016/j.bbabi.2011.11.020>
- Šlouf V, Kuznetsova V, Fuciman M, Bourcier de Carbon C, Wilson A, Kirilovsky D, Polívka T (2017) Ultrafast spectroscopy tracks carotenoid configurations in the orange and red carotenoid proteins from cyanobacteria. *Photosynth Res* 131:105–117. <https://doi.org/10.1007/s11120-016-0302-6>
- Squires AH, Dahlberg PD, Liu H, Magdaong NCM, Blankenship RE, Moerner WE (2019) Single-molecule trapping and spectroscopy reveals photophysical heterogeneity of phycobilisomes quenched by orange carotenoid protein. *Nature Comm* 10:E1172. <https://doi.org/10.1038/s41467-019-09084-2>
- Stadnichuk IN, Lukashev EP, Elanskaya IV (2009) Fluorescence changes accompanying short-term light adaptations in photosystem I and photosystem II of the cyanobacterium *Synechocystis* sp. PCC 6803 and phycobiliprotein-impaired mutants: State I/State 2 transitions and carotenoid-induced quenching of phycobilisomes. *Photosynth Res* 99:227–241. <https://doi.org/10.1007/s11120-009-9402-x>
- Stadnichuk IN, Yanyushin MF, Zhgarmukhamedov SK, Maksimov EG, Muronez EM, Paschenko VZ (2011) Quenching of phycobilisome fluorescence by orange carotenoid-protein. *Doklady Biochem Biophys* 439:167–170
- Stadnichuk IN, Yanyushin MF, Maksimov EG, Lukashev EP, Zharmukhamedov SK, Elanskaya IV, Paschenko VZ (2012) Site of non-photochemical quenching of the phycobilisome by orange carotenoid protein in the cyanobacterium *Synechocystis* sp. PCC 6803. *Biochim Biophys Acta* 1817:1436–1445. <https://doi.org/10.1016/j.bbabi.2012.03.023>
- Stadnichuk IN, Krasilnikov PM, Zlenko DV, Freidzon AY, Yanyushin MF, Rubin AB (2015) Electronic coupling of the phycobilisome with the orange carotenoid protein and fluorescence quenching. *Photosynth Res* 124:315–335. <https://doi.org/10.1007/s11120-015-0148-3>
- Staleva H, Komenda J, Shukla MK et al (2015) Mechanism of photoprotection in the cyanobacterial ancestor of plant antenna proteins. *Nat Chem Biol* 11:287–291. <https://doi.org/10.1038/nchembio.1755>
- Stoitchkova K, Zsiros O, Jávorfí T, Páli T, Andreeva A, Gombos Z, Garab G (2007) Heat- and light-induced reorganizations in the phycobilisome antenna of *Synechocystis* sp. PCC 6803. Thermooptical effect. *Biochim Biophys Acta - Bioenergetics* 1767:750–756. <https://doi.org/10.1016/j.bbabi.2007.03.002>
- Tian L, Van Stokkum I, Koehorst R, Jongerijs A, Kirilovsky D, Van Amerongen H (2011) Site, rate, and mechanism of photoprotective quenching in cyanobacteria. *J Am Chem Soc* 133:18304–18311. <https://doi.org/10.1021/ja206414m>
- Wilson A, Ajlani G, Verbavatz JM, Vass I, Kerfeld CA, Kirilovsky D (2006) A soluble carotenoid protein involved in

- phycobilisome-related energy dissipation in cyanobacteria. *Plant Cell* 18:992–1007. <https://doi.org/10.1105/tpc.105.040121>
- Wilson A, Punginelli C, Gall A, Bonetti C, Alexandre M, Routaboul J-M, Kerfeld CA, van Grondelle R, Robert B, Kennis JTM, Kirilovsky D (2008) A photoactive carotenoid protein acting as light intensity sensor. *Proc Natl Acad Sci USA* 33:2075–2080. www.pnas.org/cgi/doi/10.1073/pnas.0804636105
- Xiao C, Guo N, Liang Z, Huang Z, Li W, Xie M, Zhao F (2023) Ultrafast energy transfer dynamics in a cyanobacterial light-harvesting phycobilisome. *Processes*. <https://doi.org/10.20944/preprints202304.0938.v1>
- Zhang H, Liu H, Niedzwiedzki DM, Prado M, Jiang J, Gross ML, Blankenship RE (2014) Molecular mechanism of photoactivation and structural location of the cyanobacterial orange carotenoid protein. *Biochemistry* 53:13–19. <https://doi.org/10.1021/bi401539w>
- Zhang J, Ma J, Liu D, Qin S, Sun S, Zhao J, Sui S-F (2017) Structure of phycobilisome from the red alga *Griffithsia pacifica*. *Nature* 551:57–63. <https://doi.org/10.1038/nature24278>
- Zhao J, Jou J, Bryant DA (1992) Energy transfer process in phycobilisomes as deduced from mutational analysis. *Photosynth Res* 34:83–83
- Zheng L, Zheng Z, Li X, Wang G, Zhang K, Wei P, Zhao J, Gao N (2021) Structural insight into the mechanism of energy transfer in cyanobacterial phycobilisomes. *Nature Com* 12:5497. <https://doi.org/10.1038/s41467-021-25813-y>
- Zlenko DV, Krasilnikov PM, Stadnichuk IN (2016) Role of inter-domain cavity in the attachment of the orange carotenoid protein to the phycobilisome core and to the fluorescence recovery protein. *J Biomol Str Dyn* 34:486–496. <https://doi.org/10.1080/07391102.2015.1042913>
- Zlenko DV, Galochkina TV, Krasilnikov PM, Stadnichuk IN (2017) Coupled rows of PBS cores and PSII dimers in cyanobacteria: symmetry and structure. *Photosynth Res* 133:245–260. <https://doi.org/10.1007/s11120-017-0362-2>
- Zlenko DV, Elanskaya IV, Lukashev EP, Bolychevtseva YU, Suzina NE, Pojidaeva ES, Kononova IA, Loktyushkin AV, Stadnichuk IN (2019) Role of the PB-loop in ApcE and phycobilisome core function in cyanobacterium *Synechocystis* sp. PCC 6803. *Biochim Biophys Acta-Bioenergetics* 1860:155–166. <https://doi.org/10.1016/j.bbabi.2018.10.004>

Publisher's Note Springer Nature remains neutral with regard to jurisdictional claims in published maps and institutional affiliations.

Springer Nature or its licensor (e.g. a society or other partner) holds exclusive rights to this article under a publishing agreement with the author(s) or other rightsholder(s); author self-archiving of the accepted manuscript version of this article is solely governed by the terms of such publishing agreement and applicable law.